Heat of Adsorption of Naphthalene on Pt(111) Measured by Adsorption Calorimetry

J. Michael Gottfried,† Ebbe K. Vestergaard, Parthasarathi Bera, and Charles T. Campbell*

Department of Chemistry, Box 351700, University of Washington, Seattle, Washington 98195-1700

Received: May 1, 2006; In Final Form: June 29, 2006

The heat of adsorption of naphthalene on Pt(111) at 300 K was measured with single-crystal adsorption calorimetry. The heat of adsorption on the ideal, defect-free surface is estimated to be $(300 - 34\Theta - 199\Theta^2)$ kJ/mol. From this, a C−Pt bond energy for aromatic hydrocarbons on Pt(111) of ∼30 kJ/mol is estimated, consistent with earlier results for benzene on Pt(111). There is higher heat of adsorption at very low coverage, attributed to step sites where the adsorption heat is ≥330 kJ/mol. Saturation coverage, $\Theta = 1$ ML, corresponds to 1.55×10^{14} molecules/cm^2. Sticking probability measurements of naphthalene on Pt(111) give a high initial value of 1.0 and a Kisliuk-type coverage dependence that implies precursor-mediated sticking. The ratio of the hopping rate to the desorption rate of this precursor is ∼51. Naphthalene adsorbs transiently on top of chemisorbed naphthalene molecules with a heat of adsorption of 83−87 kJ/mol.

1. Introduction

Only recently, single-crystal adsorption calorimetry (SCAC)[1,2] has been applied to measure the heat of adsorption of a low vapor pressure organic molecule, benzene.[3,4] Here, we have employed this technique to study the adsorption of naphthalene on a Pt(111) surface.

The chemisorption of aromatic hydrocarbons (AHs) and polycyclic aromatic hydrocarbons (PAHs) on transition metal surfaces is an important topic with respect to industrial catalysis. For example, AHs and PAHs are unwanted components of fuels because they are carcinogenic and reduce the performance of diesel fuel. Furthermore, these compounds promote the emission of soot particles and larger PAHs from diesel engines.[5] These particles are considered a serious environmental and health problem. It is therefore desirable to convert AHs and PAHs to saturated hydrocarbons by catalytic hydrogenation and hydrogenolysis.[5] Both processes are performed in industry on a large scale with use of transition metal catalysts, especially platinum.[6] Studying the adsorption of naphthalene as a typical representative of this class of molecules on platinum surfaces is therefore of particular relevance with respect to heterogeneous catalysis. In this context, one of the most important parameters is the heat of adsorption of the reactant molecules, because it is a measure for the degree of interaction of the reactant with the catalyst surface. Furthermore, the heat of adsorption provides the standard enthalpies of formation of the adsorbed molecules, the key variable for determining the enthalpies and equilibrium constants for surface reactions. There are several indirect methods such as temperature programmed desorption (TPD), molecular beam relaxation spectroscopy (MBRS), and equilibrium adsorption isotherms to determine the heat of adsorption. Since the early years of the past decade, single-crystal adsorption calorimetry (SCAC)[1,2] proved to be a unique method for the direct measurement of the heats of adsorption of molecules and metal atoms. For irreversible adsorption, as in the case of naphthalene on Pt(111), it is the only technique available for a reliable measurement of the adsorption heat.

Several experimental and theoretical studies regarding naphthalene adsorption on Pt(111) have been reported.[7−17] Early studies revealed that the molecules adsorb parallel to the surface and form both ordered and disordered overlayer structures, depending on the substrate temperature.[7,9,11] LEED observations after room temperature exposure showed a diffuse 1/3-order diffraction ring. However, annealing above 100 °C resulted in an ordered overlayer with a 6×3 LEED pattern. A similar result was obtained by adsorption at elevated sample temperatures between 100 and 200 °C.[11] Later, a detailed STM investigation[13] revealed that the ordered naphthalene overlayer consists of 3×3 domains with glide-plane symmetries that lead to the observed LEED structure, a pseudo-(6×3). In these domains, the long axis of the molecules aligns with the crystallographic orientations of the metal surface. The local structure of the disordered overlayer appears to be similar to that of the ordered layer. The main differences are a higher concentration of stacking faults and smaller 3×3 domains in the disordered layer.[13] A recent study by Lavoie et al. deals with the coadsorption of naphthalene and various carbonyl compounds on Pt(111). It was found that the chemisorption induced polarization of the naphthalene molecule enhances the strength of the attractive interactions between the aromatic molecule and the carbonyl group.[14]

Naphthalene adsorption on Pt(111) has found considerable interest from the theoretical side as well. A semiempirical tight-binding calculation on Pt clusters with (111) surfaces suggested on-top adsorption with the long axis of the molecule parallel to the densely packed metal rows.[15] Density functional theory (DFT) was used to study naphthalene adsorption on a planar Pt_7 cluster.[16] According to this investigation, naphthalene adsorbs parallel to a row with one of the rings centered on a bridge site. The calculated adsorption energy is 234 kJ/mol. Recently, Morin et al.[17] performed a very detailed periodic slab DFT investigation of the adsorption of benzene, naphthalene, and anthracene on Pt(111). This study also suggests preferential adsorption of the aromatic ring systems centered on bridge sites. For the adsorption energy of naphthalene, a value of −1.37 eV (−132 kJ/mol) was calculated for a 4×3 unit cell that corresponds to $^3/_4$ of the saturation coverage.

† Present address: Lehrstuhl für Physikalische Chemie II, Universität Erlangen-Nürnberg, Egerlandstrasse 3, 91058 Erlangen, Germany.

10.1021/jp062659i CCC: $33.50
Published on Web 08/15/2006

Here, we report the first experimental measurement of the adsorption heat of naphthalene on Pt(111). This heat is used to determine the average bond energy between the aromatic C atoms of naphthalene and the Pt(111) surface. Furthermore, we use the calorimetric adsorption enthalpies of naphthalene and benzene on Pt(111) to estimate their standard enthalpies of formation on the surface.

2. Experimental Section

The SCAC apparatus, the molecular beam system (MBS), and the general experimental procedures used for these experiments have been described elsewhere.[3,4] Briefly, we employed an ultrahigh vacuum (UHV) chamber equipped with the SCAC, the MBS, and facilities for X-ray photoelectron spectroscopy (XPS), Auger electron spectroscopy (AES), low-energy ion scattering (LEIS), and low-energy electron diffraction (LEED).

Detection of the heat of adsorption is accomplished with a 9 μm thin ribbon of β-polyvinylidenfluoride (β-PVDF), a pyroelectric polymer that is coated with 50 nm layers of NiAl on both sides for electrical contact. During the calorimetric measurement, this ribbon is gently pressed to the back of the sample for thermal contact and can be retracted for sample cleaning purposes. The calorimetric measurements were performed at a sample temperature of 300 K.

The sample is a 1 μm thick Pt(111) single crystal with a diameter of 10 mm prepared by epitaxial growth on a NaCl single-crystal surface. The NaCl was dissolved in water and the crystal was mounted between two pieces of Ta foil with 8 mm diameter holes. The sample was cleaned by gentle Ar^+ sputtering followed by repeated cycles of O_2 treatment at 10^{-6} mbar and 750 K and annealing at 1100 K in UHV. After this treatment, impurities were below the Auger and XPS detection limits, and LEED showed the spots expected for Pt(111).

The MBS is pumped with a combination of turbo molecular pumps and cryo pumps. The cryo pumping is achieved by cooling the inner walls and orifices of the MBS with liquid N_2 and is especially effective for low vapor pressure compounds such as naphthalene. The naphthalene vapor (5−10 Torr) enters the MBS through a microchannel array, heated to 120 °C, to form a peaked angular distribution. After collimation by several liquid N_2 cooled orifices, the beam has a diameter of 4.23 mm at the sample position. The beam is chopped into pulses of 90 ms length with a period of 2 s before impinging on the sample. The flux is measured by means of a quartz crystal microbalance (QCM) cooled with liquid N_2. Typically, the flux per naphthalene pulse was 0.06 ML, with 1 ML (monolayer) defined throughout this paper as the saturation coverage at 300 K. Measurement of this saturation coverage, which is equivalent to 1.55×10^{14} molecules/cm^2 or 0.103 naphthalene molecules per Pt surface atom, is described below.

For calibration of the SCAC, the pulsed molecular beam is replaced by a HeNe laser. This pulsed laser beam has exactly the same diameter, pulse length, and pulse period as the molecular beam. The reflectivity of our sample at the wavelength of the HeNe laser was measured with an integrating sphere and found to be 76%. This enables us to estimate the absorbed heat from each laser pulse and use this to convert the voltage response of the ribbon into absolute energy units.

The sticking probability was measured with a line-of-sight modification of the King and Wells method as described elsewhere.[2] It provides the coverage-dependent fraction of molecules that stick to the surface and thus actually contribute to the heat signal. For practical reasons, heat and sticking probability measurements were performed in separate experiments. If adsorption is limited to the first layer and no multilayer growth occurs, the flux can be derived from the sticking measurement (in units of ML/s). By comparison with the flux measured with the QCM (in units of molecules/(cm^2 s)), the absolute saturation coverage in molecules/cm^2 per ML was calculated.

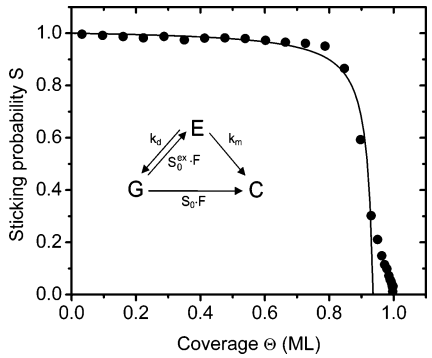

Figure 1. Sticking probability of naphthalene on Pt(111) at 300 K (circles) and best fit with the modified Kisliuk model (line). Inset: Precursor mechanism for nondissociative chemisorption without intrinsic precursor. Key: G, gas phase; C, chemisorbed state; E, extrinsic precursor; F, incident flux. The meanings of the other symbols are explained in the text.

3. Results

3.1. Sticking Probability Measurements. The sticking probability of naphthalene on Pt(111) at 300 K as a function of coverage is displayed in Figure 1. Starting from an initial value of 1.0, the sticking probability remains close to unity over a wide coverage range and drops rapidly to zero above 0.85 ML. The solid line in Figure 1 is a fit of the data with the Kisliuk model for precursor-mediated adsorption.[18,19] This model has been modified in such a way that it considers only an "extrinsic" precursor (a mobile physisorbed precursor on filled sites). Thus, the "intrinsic" precursor (a precursor on empty sites) is excluded here. Specifically, we find that molecules chemisorb with unit probability whenever they visit an empty site, thus excluding the necessity to consider any intrinsic precursor (see below). The absence of noticeable contributions to the sticking probability from intrinsic precursors has frequently been observed for chemisorption systems with extrinsic precursors (e.g., for CO on Ni(100)[20]).

According to this modified Kisliuk model, the sticking probability, S, varies with coverage, Θ, as:

$$S(\Theta) = S_0(1 - \Theta/\Theta_{max}) + \frac{S_0^{ex}\Theta(1 - \Theta/\Theta_{max})}{K + (1 - \Theta/\Theta_{max})} \quad (1)$$

with $K = k_d/k_m$. Here, S_0 and S_0^{ex} are the trapping probabilities for a molecule that strikes a clean surface site (to chemisorb) and an occupied site (to physisorb as an extrinsic precursor), respectively, and Θ_{max} is the saturation coverage of the chemisorption state. The constant K represents the ratio of the rate constants of desorption (k_d) and migration (k_m) of the precursor. The best fit of our data with the Kisliuk model (eq 1) is shown in Figure 1. This fit is weighted with the sticking probability to account for the fact that the density of data points scales with $1/S$. Without this weighting, the fit would be predominantly controlled by the data points at higher coverage. In addition, the error (of both Θ and S) increases with decreasing S, which is also compensated by weighting the fit with S. The abrupt change in slope of the experimental S vs Θ curve when

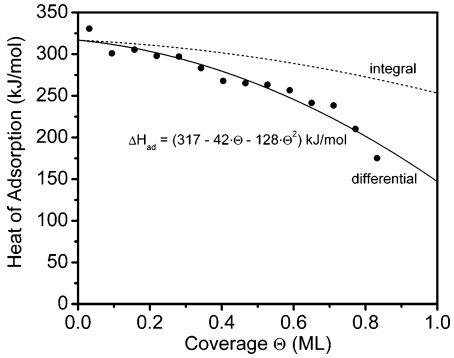

Figure 2. Differential heat of adsorption of naphthalene on Pt(111) at 300 K as a function of coverage (circles). Also displayed are the best fit of the data using a second-order polynomial dependence on coverage (solid line) and the integral heat of adsorption computed by integration of the polynomial fit (dotted line).

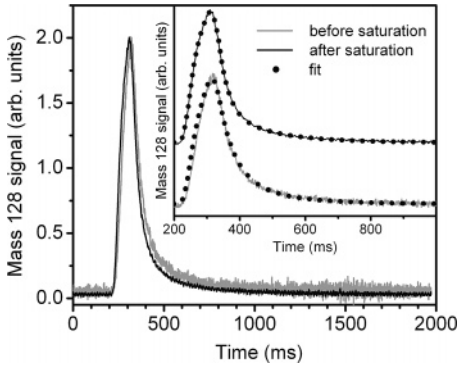

Figure 3. Naphthalene molecular beam pulses scattered from the Pt(111) surface, averaged for all pulses below 0.95 ML (gray line, smoothed by Fourier-filtering out noise above 30 Hz, and magnified) and for 30 pulses after saturation (black line, without smoothing). Inset: Comparison between the experimental pulse shapes before (gray) and after saturation (black) and the respective best fits (full circles) using the convolution integral in eq 4 with a double-exponential system function $h(t)$. See Section 3.3 for the fitting parameters. For each curve, three individual measurements under identical conditions were averaged to improve the signal-to-noise ratio.

$\Theta \sim 0.93$ in Figure 1 clearly indicates that different adsorption kinetics dominate at higher coverages. Therefore, we have omitted all data points where S is less than 0.30 and treated the maximum coverage of the chemisorbed state, Θ_{max}, as a fitting parameter. From the best fit, we derive $S_0 = S_0^{ex} = 1$, $K = 0.0195$, and $\Theta_{max} = 0.936$.

The value for $K = k_d/k_m$ shows that, on average, $1/0.0195 \approx 51$ hopping events occur before a precursor molecule desorbs. For benzene on Pt(111), this value was found to be ≈28 hops, also at 300 K.[3] The continued, slower adsorption above $\Theta_{max} = 0.936$ could be attributed to very slow diffusion of chemisorbed naphthalene, which occasionally opens up another Pt site large enough to chemisorb another naphthalene molecule. Consistent with this interpretation, the heat measurements below prove that chemisorbed naphthalene molecules have very limited mobility on the time scale of these measurements. However, their occasional movement at 300 K has been seen in repeated STM images.[13]

By dividing the absolute flux measurement of the QCM by the flux in ML/s from the sticking probability measurements, the naphthalene saturation coverage (i.e., $\Theta = 1$) is found to be 1.55×10^{14} molecules/cm^2 at 300 K. This value corresponds to 0.103 naphthalene molecules per Pt surface atom, and compares reasonably well to $^1/_9 = 0.111$ molecules per Pt atom in the ideal 3×3 structure.

3.2. Heat of Adsorption Measurements. Figure 2 shows the molar heat of adsorption of naphthalene on Pt(111) at 300 K as a function of coverage. These heats were calculated from the measured absolute calorimetric heats by averaging over 7 individual measurements, dividing by the number of moles adsorbed in each pulse (given by flux times pulse duration times sticking coefficient), and adding $RT_{source}/2$, as described previously.[2] The temperature of the source, T_{source}, and thus the temperature of the molecules impinging on the sample, is 393 K, which deviates from the sample temperature of 300 K. Therefore, we had to take the additional contribution from the extra thermal energy of the gas molecules into account. We estimated this heat contribution by integrating the experimental C_p vs T curve[21] between sample and source temperature. The resulting heat, 14.8 kJ/mol, was subtracted from the data. The thus corrected heat of adsorption is plotted vs coverage in Figure 2. It is equal to the standard (1 bar) molar enthalpy of adsorption and the isosteric differential heat of adsorption. We estimate the maximum error in the absolute values of these heats as ≈10%. The main error sources are the uncertainties in the beam flux measurement and in the optical reflectivity of the sample.

Figure 2 shows that the heat of adsorption decreases with coverage. We attribute this decrease to repulsive lateral interactions between the adsorbed naphthalene molecules and to a change of the adsorption site with increasing coverage (see discussion below). The solid line is a second-order polynomial fit of the experimental data and is described by the equation:

$$\Delta H_{ad} = (317 - 42\Theta - 128\Theta^2)\ \text{kJ/mol} \qquad (2)$$

where the coverage (Θ) is in units of ML. Also displayed in Figure 2 is the integral heat of adsorption, obtained by integrating the polynomial fit of the differential heat. Extrapolation of the polynomial fit to zero coverage gives an initial heat of adsorption of 317 kJ/mol. The first pulse leads to a significantly higher adsorption heat, 331 kJ/mol, than the following pulses, which is probably due to the initial adsorption on defect sites (see below). The main defects on Pt(111) samples prepared in this way are step edges. Extrapolation to saturation coverage results in a heat of adsorption of 147 kJ/mol at $\Theta = 1$ ML. Excluding the first data point from the fit leads to slightly different parameters as shown in eq 3:

$$\Delta H_{ad} = (300 - 34\Theta - 199\Theta^2)\ \text{kJ/mol} \qquad (3)$$

This equation is probably more truly representative for the perfect Pt(111) surface.

3.3. Transient Sticking after Saturation. Analysis of the mass spectrometer signal after saturation reveals that a large fraction of the naphthalene molecules is transiently adsorbed and desorbs over the 2 s period between the pulses (Figure 3). The heat of adsorption of this transiently adsorbed species can be estimated by analyzing the shape of the mass spectrometer signal. For this purpose, the signal was fitted with a convolution integral:

$$s(t) = \int_0^\theta i(t - t')h(t')\,dt' \qquad (4)$$

where $s(t)$ is the measured signal at time t, $i(t)$ is the instrument response function, θ is the period of the pulses ($\theta = 2$ s), and $h(t)$ is the system function that describes the actual adsorption/desorption process. The function $i(t)$ accounts for the fact that the molecular beam pulse is not infinitely short, but extends

over 90 ms during which desorption already occurs.[4] This function was measured by directing the molecular beam directly into the mass spectrometer and averaging over 100 pulses. (A very similar response time was also seen for molecules scattering off a hot gold surface.) Using a single exponential for the system function $h(t)$ resulted in a bad agreement between the fit and experimental curves, while the following double exponential decay function provided an excellent fit to the experimental curve (Figure 3, inset): $h(t) = A_{a1} \exp(-t/\tau_{a1}) + A_{a2} \exp(-t/\tau_{a2})$, with $A_{a1} = 0.055$ and $A_{a2} = 0.0077$ (in units of the normalized mass spectrometer signal), and $\tau_{a1} = 0.029$ s and $\tau_{a2} = 0.14$ s. This result implies that the sticking probability during the entire duration of the gas pulse remains constant and that 60% of the transiently adsorbed molecules after saturation have characteristic residence times of 0.029 s and 40% of 0.14 s. The presence of two lifetimes suggests heterogeneity in the sites visited by these molecules, possibly due to defects such as step edges or heterogeneity in surface packing of the underlying monolayer, even at saturation.

Figure 3 reveals that the mass spectrometer pulses *before* saturation also show an exponential tail, indicating that transient adsorption also occurs at submonolayer coverages. For comparison with the data above, the averaged pulses were normalized (i.e., scaled up to compensate for the lower intensity of the submonolayer signals) and fitted with the same convolution integral in eq 4 as employed for the postsaturation pulses. Again, an excellent agreement between fit and experimental curve was obtained with a double exponential function $h(t)$ and the parameters $A_{b1} = 0.037$ and $A_{b2} = 0.0077$ (again in the units of the normalized mass spectrometer signal), and $\tau_{b1} = 0.045$ s and $\tau_{b2} = 0.14$ s (Figure 3, inset). Both residence times are very close to the values measured after saturation, which implies that the nonsticking fraction before saturation sampled the same types of sites on the surface as after saturation: sites on the Pt surface that are already covered by chemisorbed naphthalene molecules. The nonsticking fraction can therefore be identified with molecules that transiently adsorb in the extrinsic precursor state. This result also supports our previous assumption (see section 3.1) that naphthalene adsorption on Pt(111) is not mediated by an intrinsic precursor state, since none of the transiently adsorbed molecules show much longer residence times at low coverage. The slightly longer residence time of the larger component of the double exponential before saturation as compared to the situation after saturation reflects the fact that the transiently trapped molecules bind slightly more strongly before saturation, possibly due to partial orbital overlap with small patches of the surface that are still naphthalene free.

The above analysis of the pulse line shape is based on the assumption that the trapping probability is independent of coverage within the coverage increase caused by a single pulse ($\Delta\Theta \approx 0.06$ ML). The excellent agreement between fit and experimental curves, especially after saturation, proves that this assumption is very well justified.

4. Discussion

The coverage dependence of the adsorption heat can be described by the second-order polynomial in eq 2. According to Persson,[22] this functional dependence can be explained with a simple lattice site model for *immobile* adsorbates with pairwise interactions between the molecules. In this model, the chemisorbed molecules cannot diffuse (i.e., they essentially stay where they initially stick and thus establish a random distribution across the surface, rather than their lowest energy distribution). However, they are allowed to move slightly out of the site centers to relax nearest-neighbor repulsion, which may result from direct steric interactions or dipole−dipole interactions. However, this relaxation mechanism becomes less effective as the coverage increases, because the constraints imposed by neighboring molecules prevent the necessary movements. Considering a hexagonal lattice with only nearest-neighbor interactions, our initial heat of adsorption of 317 kJ/mol equals Perrson's parameter μ, the adsorption energy of an isolated naphthalene molecule. The first-order coefficient in eq 2, 42 kJ/mol, equals Perrson's $6(V_0 - 2\epsilon)$, and the second-order coefficient, 128 kJ/mol, equals 12ϵ. With this model, we obtain $V_0 = 28.2$ kJ/mol for the pairwise repulsion between two molecules centered on nearest-neighbor sites and $\epsilon = 10.6$ kJ/mol for the reduction of the total energy per molecule that occurs when two neighboring molecules reduce their repulsion by slightly moving out of their site centers.

Compared to benzene ($V_0 = 21.8$ kJ/mol, $\epsilon = 6.9$ kJ/mol),[3] we find here a higher value for V_0, which is plausible considering the larger size of the naphthalene molecules. We also find a higher value for ϵ, which seems to scale roughly with the number of C atoms.

Note that lack of mobility in the model used to fit the heat data for $\Theta < 0.85$ does not rule out the very slow mobility suggested by the sticking probability for $\Theta > 0.94$ (Figure 1), since the time scale for the latter measurements is longer (due to the lower sticking probability there).

Our experimental heat of adsorption can be used to estimate the standard heat of formation of naphthalene on Pt(111). Using the gas-phase standard enthalpy of formation of naphthalene, 150.6 kJ/mol,[23] we obtain a value of −166 kJ/mol in the limit of zero coverage (or, with eq 3 under exclusion of the first pulse, −149 kJ/mol). For comparison, benzene on Pt(111) at zero coverage has a standard heat of formation of −114 kJ/mol as can be estimated from the heat of adsorption, 197 kJ/mol,[3] and the gas-phase standard heat of formation, 82.9 kJ/mol.[24]

The heat of adsorption can also be employed to calculate the average bond energy between an sp^2 hybridized aromatic C atom in the naphthalene molecule and the Pt(111) surface. It is well established that naphthalene adsorbs molecularly on Pt(111) at 300 K with the molecular plane parallel to the surface.[13] Thus, the initial heat of adsorption equals the sum of the bond energies between 10 aromatic C atoms in the molecule and the surface. This Pt−C bond is viewed as a σ donor bond between the sp^2 orbitals on the C atoms and unoccupied Pt orbitals, combined with some π back-bonding, where these sp^2 orbitals are still dominated by their intramolecular C−C π bonding in the aromatic ring. The average bond energy is 317/10 kJ/mol ≈ 32 kJ/mol. Within the margins of error of our measurement, this value is identical with the average Pt−C bond energy found for benzene,[3] 33 kJ/mol. If we exclude the first pulse, which is probably influenced by adsorption on defect sites, from the extrapolation to zero coverage and use the second-order polynomial fit in eq 3, the initial adsorption heat is reduced to 300 kJ/mol. This value may be more representative for adsorption on regular terrace sites than the value of 317 kJ/mol. With the smaller initial adsorption heat, we obtain an average C(sp^2)−Pt bond energy of 30 kJ/mol, which is 10% lower than in the case of benzene on Pt.

It has been claimed that chemisorption of planar aromatic molecules on metal surfaces can be accompanied by distortion-induced rehybridization,[25] which means that the hybridization state of the C atoms of adsorbed naphthalene may deviate from sp^2. In particular, NEXAFS measurements on benzene/Pt(111) by Mainka et al.[25] showed that the π^* resonance of benzene

does not vanish for s-polarized light as required by the dipole selection rules for a molecule that is planar and adsorbed with the molecular plane parallel to the surface. The authors concluded that these transitions become allowed because of out-of-plane molecular distortions. This argument is further supported by Hartree−Fock calculations showing that the H atoms can be bent upward by up to 40°, which would indeed indicate sp^3 rather than sp^2 hybridization.[25] However, the weak bonding found in our experiments seems inconsistent with sp^3 hybridization, since this would lead to much stronger regular C−Pt σ bonds to the surface. For C−Pt σ bonds in systems where the C atoms are truly sp^3 hybridized, such as di-σ bonded ethylene on Pt(111), bond energies of ≈250 kJ/mol per C atom have been measured by King's group,[1,26,27] whereas our measured bond energy is only $\sim 1/8$ of this. Therefore, the hybridization state of carbon in adsorbed benzene and naphthalene is clearly very different from sp^3 and probably closer to sp^2.

However, a small deviation from sp^2 hybridization may account for the fact that the adsorption heat per C atom is lower for naphthalene (30 kJ/mol) than for benzene (33 kJ/mol). In adsorbed naphthalene, the two carbon atoms (9, 10) shared by both rings are certainly sp^2 hybridized, because otherwise the carbon framework of the molecule would lose its planarity. The other eight carbon atoms (1−8) can more strongly deviate from sp^2 by bending their hydrogens upward. If we assume that C atoms 1−8 have the same adsorption energy per atom as in benzene, then the other two atoms (9, 10) contribute only 18 kJ/mol each to the total initial adsorption energy of naphthalene. This value may be associated with the adsorption energy of truly sp^2 hybridized carbon on Pt(111). There are other possible causes for the slightly smaller average bond energy per carbon atom of naphthalene, as for example the better average registry of the C atoms with the underlying Pt atom lattice for the smaller benzene molecule.

To compare our experimental heats of adsorption with theoretical results, we have to use our integral heats at the coverage used for the calculation. The DFT calculations by Morin et al. for a 3 × 4 structure of naphthalene on Pt(111) gave a value of only 132 kJ/mol,[17] which is less than half of our integral heat of 272 kJ/mol at the corresponding coverage of 0.8 ML (with respect to our relative scale, see below).

Comparison of our adsorption heat of naphthalene with the respective values for benzene[3,17] and anthracene[17] provides information about how the adsorption heat depends on the number of C atoms in the aromatic system. In Figure 4, the available experimental and theoretical values[17] are plotted vs the number of aromatic C atoms. This plot reveals that the adsorption heat scales almost linearly with the number of C atoms for both experimental and theoretical values. However, we find two major differences between experiment and theory: First, theory underestimates the heats by more than a factor of 2. Second, extrapolation of the experimental values to zero C atoms ($n = 0$) results in a vanishing adsorption heat, whereas theory predicts a nonzero offset of 23 kJ/mol. The general formula for the investigated aromatic hydrocarbons, $C_nH_{n/2+3}$, suggests a possible interpretation of this nonzero offset in the computational data. For $n = 0$, a formal fragment "H_3" remains and the offset could be related to its adsorption heat. Our experiment, however, does not confirm the existence of this offset. We note that, for benzene adsorption on Pt(111), other adsorption heats, which are closer to the experimental value (but still much lower), have been computed (in kJ/mol): 132,[28] 117,[29] 104,[30] and 102.[31] The fact that all these studies underestimate the heat of adsorption suggests fundamental

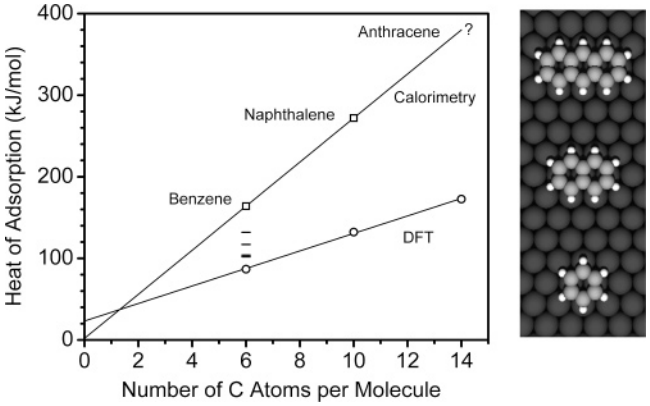

Figure 4. Comparison of the experimental integral heats of adsorption of benzene[3] and naphthalene on Pt(111) (squares) and the computational results[17] (circles) at the same coverages. The lines are the best linear fits of the respective data sets and follow the equations $(11n_C + 23)$ kJ/mol for DFT and $(27n_C + 2)$ kJ/mol for calorimetry (with n_C the number of C atoms). The horizontal bars show further computed benzene adsorption energies.[28−31]

problems connected with DFT calculations for aromatic hydrocarbons adsorbed on metal surfaces. Similar problems seem to arise in the calculation of adsorption geometries and bond properties, as indicated by a controversy about DFT calculations on PTCDA/Ag(111).[32−34] More successful was the recent application of a wave function based ab initio approach to benzene adsorbed on Cu(111).[35] In these calculations, London dispersion forces were considered explicitly on the level of Møller−Plesset perturbation theory (MP2), which led to remarkable accuracy of the adsorption energy and other quantities. It is well-known that DFT treats dispersion forces poorly. Given the weakness of the bonds here (30 kJ/mol, compared to ≈250 kJ/mol for typical C−Pt σ bonds[1,26,27]), it is likely that dispersion forces make a major contribution. Our results provide a benchmark for testing theoretical approaches for treating aromatic adsorbates on a metal surface like Pt that makes stronger bonds than Cu to these molecules.

Our experimental saturation coverage, 1.55×10^{14} molecules/cm^2, is about 7% lower than the saturation coverage for a 3 × 3 overstructure, 1.67×10^{14} molecules/cm^2, which suggests that no perfect 3 × 3 structure is formed under our experimental conditions. This conclusion is in agreement with previous LEED observations, which show that a 3 × 3 structure develops only at elevated temperature around 373 K, whereas adsorption at room temperature leads to a disordered layer.[11] An STM study on both ordered and disordered layers revealed that the disordered layer has a higher concentration of stacking faults and consists of smaller 3 × 3 domains,[13] although the structures are essentially similar. Therefore, our lower saturation coverage is probably due to the higher concentration of faults in the layer formed by adsorption at 300 K, resulting from lack of adsorbate mobility. This is consistent with the fact that the shape of the heat curve (Figure 2) implies that adsorbed naphthalene molecules are immobile at 300 K on Pt(111) (see above).

Figure 2 shows that the first pulse has significantly higher adsorption energy than the following pulses, probably due to initial adsorption on defects. It is likely that only a fraction of the first pulse is needed to saturate the defect sites and that the other molecules in the pulse adsorb on regular sites. This means that the adsorption heat on the defects may be even higher than the measured 331 kJ/mol for the first pulse, depending on the actual defect density. Since the dominant defect on such a Pt(111) surface is well-known to be step edges, and since step edges are known to bind benzene molecules more strongly than

terraces on Cu(111),[36] we attribute this to step edges. We conclude that the adsorption heat on steps (≥331 kJ/mol) is >10% higher than the initial adsorption heat on terrace sites (~300 kJ/mol).

Our attribution of the higher heat of adsorption in the first pulse to preferential population of steps seems to be contradictory to the lack of mobility used in modeling the coverage dependence of the heat, above, and the direct STM observation of very slow mobility of adsorbed naphthalene on Pt(111) at 300 K.[13] The initial population of steps must therefore be attributed to transient mobility when the molecule is not yet fully chemisorbed in the perfect geometry (e.g. edge-on). Also, it is possible that not all the step sites are populated in the first pulse, so diffusion may still be a limiting factor.

In Section 3.3, we also determined the characteristic residence times for the transient adsorption of naphthalene before and after saturation. These values equal the inverse of the respective desorption rate constant ($k_i = 1/\tau_i$), and can be used to derive the desorption activation energies $E_{\mathrm{des},i}$ by means of the Arrhenius equation $k_i = \nu_{\mathrm{des},i} \exp(-E_{\mathrm{des},i}/kT)$. First, we focus on the transient adsorption *after* saturation. Assuming a pre-exponential factor (or prefactor) of $\nu_{\mathrm{des}} = 10^{13}\ \mathrm{s}^{-1}$, we obtain $E_{\mathrm{des,a1}} = 65.9$ kJ/mol and $E_{\mathrm{des,a2}} = 69.8$ kJ/mol from the two lifetimes. Both values are below the sublimation enthalpy of naphthalene, $\Delta H_{\mathrm{sub}} = 72.32$ kJ/mol,[37] which is an unlikely result and suggests that the assumed prefactor is too low. Indeed, for larger hydrocarbon molecules, desorption prefactors much higher than $10^{13}\ \mathrm{s}^{-1}$ have been observed. For example, Tait et al. found a prefactor of $10^{19}\ \mathrm{s}^{-1}$ for the desorption of *n*-decane ($C_{10}H_{22}$) from a MgO(100) surface.[38] Reasonable upper and lower limits for the desorption energy of the transiently adsorbed molecules are the heat of adsorption at saturation coverage, $\Delta H_{\mathrm{ad,sat}} = 147$ kJ/mol, and the sublimation enthalpy, respectively. Using τ_1 for the calculation, the estimated prefactors are 2.25×10^{14} and $1.35 \times 10^{27}\ \mathrm{s}^{-1}$ for $E_{\mathrm{des}} = \Delta H_{\mathrm{sub}}$ and $\Delta H_{\mathrm{ad,sat}}$, respectively. We expect the true prefactor to be somewhere between these two limiting values, but probably closer to the lower one.

For a better estimate of the prefactor and, therefore, of the transient precursor's adsorption energy, we employed transition state theory (TST),[19,39] according to which the desorption prefactor is given by:

$$\nu_{\mathrm{des}} = \frac{k_{\mathrm{B}}T}{h}\frac{q^{\ddagger}}{q_{\mathrm{ad}}} \tag{5}$$

(with the temperature T, the Boltzmann constant k_{B}, Planck's constant h, and the partition functions for the transition state, $q^{\ddagger}$, and for the adsorbate, q_{ad}). An accurate calculation of the partition functions would require detailed knowledge of the interaction potentials of the adsorbed molecule and the transition state. These data are not available. Nevertheless, we can determine upper and lower limits for the prefactor based on reasonable assumptions about the degrees of freedom in the adsorbed state and the transition state. Specifically, we neglect all vibrational contributions in the partition function, which are small contributions and mostly cancel in eq 5. We assume that the transition state can be described as a free gas-phase molecule with three rotational and two translational degrees of freedom, i.e., with the model of a three-dimensional rigid rotator, in which the translational motion perpendicular to the surface represents the critical degree of freedom and is not considered in $q^{\ddagger}$. Therefore, the partition function of the transition state can be calculated as:

$$q^{\ddagger} = q_{\mathrm{tr,2D}}{}^{\ddagger} q_{\mathrm{rot,3D}}{}^{\ddagger} \tag{6}$$

The translational partition function in two dimensions, $q_{\mathrm{tr,2D}}{}^{\ddagger}$, is[40]

$$q_{\mathrm{tr,2D}}{}^{\ddagger} = \frac{2\pi m k_{\mathrm{B}} T A}{h^2} \tag{7}$$

where A is the area occupied by one naphthalene molecule in the saturated layer, $A = 6.45 \times 10^{-19}\ \mathrm{m}^2$, and m is the mass of the molecule.

The rotational partition function in three dimensions, $q_{\mathrm{rot,3D}}{}^{\ddagger}$, is expressed as[40]

$$q_{\mathrm{rot,3D}}{}^{\ddagger} = \frac{\pi^{1/2}}{\sigma}\left(\frac{k_{\mathrm{B}}T}{hc_0}\right)^{3/2}(B_{\mathrm{A}}B_{\mathrm{B}}B_{\mathrm{C}})^{-1/2} \tag{8}$$

with the symmetry factor σ ($\sigma = 4$ for naphthalene), the velocity of light c_0, and the rotational constants B_{A}, B_{B}, and B_{C} for naphthalene (in m^{-1}).[41]

Now, we consider two limiting cases for the state of the adsorbate. In the completely *mobile* limit, the adsorbate molecule is assumed to possess two translational degrees of freedom parallel to the surface and one rotational degree of freedom around an axis perpendicular to the molecular plane, which is assumed to be parallel to the surface. The partition function for this rotation around a fixed axis, $q_{\mathrm{rot,1D}}$, is given by the expression:

$$q_{\mathrm{rot,1D}} = \frac{\pi^{1/2}}{\sigma}\left(\frac{k_{\mathrm{B}}T}{hc_0B_{\mathrm{A}}}\right)^{1/2} \tag{9}$$

where B_{A} is the rotational constant for the rotation around the axis perpendicular to the molecular plane. The translational partition function for the mobile adsorbate is identical to $q_{\mathrm{tr,2D}}{}^{\ddagger}$, which is given by eq 7. Therefore, the translational contributions cancel and the prefactor for the mobile limit depends only on the rotational partition functions:

$$\nu_{\mathrm{mobil}} = \frac{k_{\mathrm{B}}T}{h}\frac{q_{\mathrm{rot,3D}}{}^{\ddagger}}{q_{\mathrm{rot,1D}}} \tag{10}$$

The opposite limit is represented by a completely *immobile* adsorbate with no rotational or translational degrees of freedom. In this case, the prefactor ν_{immobile} depends only on the partition function of the transition state and can be expressed as:

$$\nu_{\mathrm{immobil}} = \frac{k_{\mathrm{B}}T}{h} q_{\mathrm{tr,2D}}{}^{\ddagger} q_{\mathrm{rot,3D}}{}^{\ddagger} \tag{11}$$

The prefactors for the two limiting cases, along with the corresponding desorption activation energies of the transiently adsorbed species before (b1, b2) and after (a1, a2) saturation, are summarized in Table 1.

Compared to our previous estimate, according to which the range of possible values for E_{des} was limited by ΔH_{sub} and $\Delta H_{\mathrm{ad,sat}}$, the energy values presented in Table 1 now cover a much smaller range. Moreover, considering that the activation energy for surface diffusion rarely exceeds 20% of the desorption activation energy, it is reasonable to assume that the adsorbate is close to the *mobile* limit. The respective desorption energies after saturation for the mobile limit, 83−87 kJ/mol, are close the sublimation enthalpy of 73.6 kJ/mol and are much lower than the adsorption heat extrapolated to saturation using

TABLE 1: Theoretical Pre-exponential Factors and Resulting Desorption Energies of the Transiently Adsorbed Fraction at 300 K, for the Limits of Mobile and Immobile Adsorbates

	τ in s	mobile adsorbate	immobile adsorbate
ν_{des}/s^{-1}		1.0×10^{16}	6.1×10^{21}
E_a (kJ/mol)			
a1	0.029	83	105
a2	0.14	87	109
b1	0.045	84	118
b1	0.14	87	109

eq 2, 147 kJ/mol. This is a difference to our findings for benzene on this surface,[3] where the transient desorption energy was close to the adsorption heat at saturation. This difference, however, could arise from errors in extrapolating the data in Figure 2 to saturation coverage. Note that eq 3 extrapolates instead to only 67 kJ/mol. The desorption energies of the transiently adsorbed naphthalene molecules *before* saturation, 84−87 kJ/mol, are very similar to the respective values *after* saturation, which reflects our observation above that the transiently adsorbed molecules before saturation visit the same type of sites on the surface as after saturation: sites already occupied by chemisorbed molecules.

5. Conclusions

The heat of adsorption of naphthalene on Pt(111) decreases with coverage as $(317 - 42\Theta - 128\Theta^2)$ kJ/mol. The standard heat of formation of naphthalene on Pt(111) is −166 kJ/mol at zero coverage. These values also include contributions from step sites, where the heat of adsorption is ≥330 kJ/mol. More truly representative for the heat of adsorption on regular terrace sites is the equation $(300 - 34\Theta - 199\Theta^2)$ kJ/mol, obtained by excluding the lowest coverage data point, which is influenced by adsorption on defects. With this equation, the average bond energy of the C(sp^2)−Pt bond is ≈30 kJ/mol and the standard heat of formation of naphthalene on Pt(111) is −149 kJ/mol, both at zero coverage. Saturation coverage corresponds to 1.55×10^{14} molecules/cm^2, which is 7% lower than expected for the ideal 3×3 structure. The sticking probability of naphthalene at 300 K has a high initial value of 1.0 and decreases with a Kisliuk-type behavior as the coverage increases, implying precursor-mediated adsorption. The ratio of the hopping rate to the desorption rate of this precursor is ≈51. After completion of the first layer, naphthalene adsorbs transiently on the saturated surface with a heat of adsorption of 83−87 kJ/mol and desorbs with a prefactor of $10^{19\pm3}$ s^{-1}. The Kisliuk precursor before saturation has a very similar adsorption energy and prefactor.

Acknowledgment. We acknowledge the National Science Foundation for support of this work. J.M.G. thanks the Alexander von Humboldt Foundation for a Feodor Lynen Fellowship. E.K.V. acknowledges support from the Danish Research Agency (Grant no. 272-05-0061). We thank J. Chevallier at Aarhus University in Denmark for kindly providing the platinum single crystal. We appreciate the support by the staff of the Chemistry machine shop (B. Holm, J. Heutink, E. McArthur) and electronics shop (J. Gladden, L. Buck, B. Beaty, R. Olund).

References and Notes

(1) Brown, W. A.; Kose, R.; King, D. A. *Chem. Rev.* **1998**, *98*, 797.
(2) Stuckless, J. T.; Frei, N. A.; Campbell, C. T. *Rev. Sci. Instrum.* **1998**, *69*, 2427.
(3) Ihm, H.; Ajo, H. M.; Gottfried, J. M.; Bera, P.; Campbell, C. T. *J. Phys. Chem. B* **2004**, *108*, 14627.
(4) Ajo, H. M.; Ihm, H.; Moilanen, D. E.; Campbell, C. T. *Rev. Sci. Instrum.* **2004**, *75*, 4471.
(5) Cooper, B. H.; Donnis, B. B. L. *Appl. Catal. A* **1996**, *137*, 203.
(6) Du, H. B.; Fairbridge, C.; Yang, H.; Ring, Z. *Appl.Catal. A* **2005**, *294*, 1.
(7) Gland, J.; Somorjai, G. A. *Surf. Sci.* **1973**, *38*, 157.
(8) Firment, L. E.; Somorjai, G. A. *J. Chem. Phys.* **1975**, *63*, 1037.
(9) Firment, L. E.; Somorjai, G. A. *Surf. Sci.* **1976**, *55*, 413.
(10) Firment, L. E.; Somorjai, G. A. *Surf. Sci.* **1979**, *84*, 275.
(11) Dahlgren, D.; Hemminger, J. C. *Surf. Sci.* **1981**, *109*, L513.
(12) Dahlgren, D.; Hemminger, J. C. *Surf. Sci.* **1982**, *114*, 459.
(13) Hallmark, V. M.; Chiang, S.; Brown, J. K.; Wöll, C. *Phys. Rev. Lett.* **1991**, *66*, 48.
(14) Lavoie, W.; McBreen, P. H. *J. Phys. Chem. B* **2005**, *109*, 11986.
(15) Gavezotti, A.; Ortoleva, E.; Simonetta, M. *Chem. Phys. Lett.* **1983**, *98*, 536.
(16) de Souza, P. R. N.; Aranda, D. A. G.; Carneiro, J. W. D.; de Oliveira, C. D. B.; Antunes, O. A. C.; Passos, F. B. *Intl. J. Quantum Chem.* **2003**, *92*, 400.
(17) Morin, C.; Simon, D.; Sautet, P. *J. Phys. Chem. B* **2004**, *108*, 12084.
(18) Kisliuk, P. *J. Phys. Chem. Solids* **1957**, *3*, 95.
(19) Masel, R. I. *Principles of Adsorption and Reaction of Solid Surfaces*; John Wiley & Sons: New York, 1996; pp 599−603.
(20) D'Evelyn, M. P.; Steinrück, H.-P.; Madix, R. J. *Surf. Sci.* **1987**, *180*, 47.
(21) *Selected Values of Properties of Chemical Compounds*; Thermodynamics Research Center, Texas A&M University: College Station, TX, 1997.
(22) Persson, B. N. J. *Surf. Sci.* **1991**, *258*, 451.
(23) Coleman, D. J.; Pilcher, G. *Trans. Faraday Soc.* **1966**, *62*, 821.
(24) Prosen, E. J.; Gilmont, R.; Rossini, F. D. *J. Res. Natl. Bur. Stand.* **1945**, *34*, 65.
(25) Mainka, C.; Bagus, P. S.; Schertel, A.; Strunskus, T.; Grunze, M.; Wöll, C. *Surf. Sci.* **1995**, *341*, L1055.
(26) Yeo, Y. Y.; Stuck, A.; Wartnaby, C. E.; King, D. A. *Chem. Phys. Lett.* **1996**, *259*, 28.
(27) Gross, H.; Campbell, C. T.; King, D. A. *Surf. Sci.* **2004**, *572*, 179.
(28) Morin, C.; Simon, D.; Sautet, P. *J. Phys. Chem. B* **2003**, *107*, 2995.
(29) Saeys, M.; Reyniers, M. F.; Marin, G. B.; Neurock, M. *J. Phys. Chem. B* **2002**, *106*, 7489.
(30) Saeys, M.; Reyniers, M. F.; Neurock, M.; Marin, G. B. *J. Phys. Chem. B* **2003**, *107*, 3844.
(31) Saeys, M.; Reyniers, M. F.; Neurock, M.; Marin, G. B. *J. Phys. Chem. B* **2005**, *109*, 2064.
(32) Hauschild, A.; Karki, K.; Cowie, B. C. C.; Rohlfing, M.; Tautz, F. S.; Sokolowski, M. *Phys. Rev. Lett.* **2005**, *94*, 036106.
(33) Rurali, R.; Lorente, N.; Ordejon, P. *Phys. Rev. Lett.* **2005**, *95*, 209601.
(34) Hauschild, A.; Karki, K.; Cowie, B. C. C.; Rohlfing, M.; Tautz, F. S.; Sokolowski, M. *Phys. Rev. Lett.* **2005**, *95*, 209602.
(35) Bagus, P. S.; Hermann, K.; Wöll, C. *J. Chem. Phys.* **2005**, *123*, 184109.
(36) Stranick, S. J.; Kamna, M. M.; Weiss, P. S. *Surf. Sci.* **1995**, *338*, 41.
(37) Torres-Gomez, L. A.; Barreiro-Rodriguez, G.; Galarza-Mondragon, A. *Thermochim. Acta* **1988**, *124*, 229.
(38) Tait, S. L.; Dohnalek, Z.; Campbell, C. T.; Kay, B. D. *J. Chem. Phys.* **2005**, *122*, 164708.
(39) Eyring, H. *J. Chem. Phys.* **1935**, *3*, 107.
(40) Hill, T. L. *Statistical Thermodynamics*; Addison-Wesley Publishing Company, Inc.: Reading, MA, 1960.
(41) Kabir, M. H.; Kasahara, S.; Demtroder, W.; Tatamitani, Y.; Doi, A.; Kato, H.; Baba, M. *J. Chem. Phys.* **2003**, *119*, 3691.